

## Secondary Electron Emission from Clean Surface of Molybdenum Due to Low-Energy Noble Gas Ions\*

P. MAHADEVAN, J. K. LAYTON, AND D. B. MEDVED

*Space Science Section, General Dynamics/Astronautics, San Diego, California*

(Received 7 August 1962)

Secondary electron yields from clean, polycrystalline, molybdenum bombarded by  $\text{He}^+$  and  $\text{Ar}^+$  have been measured for the kinetic energy range 100 eV to 2.5 keV. This covers the transition energy region where electron ejection processes depending on the translational energy of the bombarding particle are superposed on those depending on their potential energies. A definite kinetic energy threshold for electron ejection is observed for  $\text{He}^+$  at about 500 eV and for  $\text{Ar}^+$  at about 700 eV. For  $\text{He}^+$ , the yield drops as the energy increases to about 500 eV and, thereafter, increases linearly with energy. In the case of  $\text{Ar}^+$   $\gamma$  is relatively insensitive to beam energy up to the kinetic threshold and, thereafter, increases linearly. The agreement between the observed variation of  $\gamma$  with ion kinetic energy and a theoretical calculation of the same is discussed.

### INTRODUCTION

THERE exists a considerable gap in ion energy for which reliable measurement of secondary electron yields from various clean target materials is not available. Using low-energy (10 eV to 1 keV) ions of the noble gases, Hagstrum<sup>1</sup> has studied secondary electron emission from clean metallic and semiconductor surfaces under ultra-high vacuum. Telkovskii,<sup>2</sup> using comparable vacuum conditions and techniques has investigated the energy range from a few keV to 100 keV, for ions and neutral atoms. The same energy range has been covered for hydrogen ions by Large and Whitlock<sup>3</sup> using reasonably clean targets. However, in the transition energy region extending from a few hundred to a few thousand eV where electron ejection processes depending on the translational energy of the bombarding particle are superposed on those depending on their potential energies, comparable measurements have not been reported. This paper presents results on secondary electron emission from clean Mo bombarded by  $\text{He}^+$  and  $\text{Ar}^+$  in the energy range 100 eV, to 2.5 keV. This energy range covers the transition from purely potential to kinetic energy dependence of secondary electron emission for most systems.

### THE APPARATUS

#### Vacuum System

A schematic diagram of the vacuum assembly is given in Fig. 1. The pressures correspond to operating conditions with source gas flowing. It consists essentially of a source chamber, a differentially pumped buffer chamber, and an out-bakeable main target chamber with a working volume of 2 cu ft. Soft aluminum gaskets are used for the bakeable part of the system,

provision being made to differentially pump the region between the double-knife edge seals on both sides of each gasket.

Continuous pumping for about two days brings the target chamber pressure down to about  $2 \times 10^{-9}$  Torr without baking. If the system is baked out at 200°C for 24 h, the pressure goes down to about  $8 \times 10^{-10}$  Torr. The background pressures in the source and buffer chambers are about  $10^{-7}$  Torr. All pressures are measured with Veeco RG-21A ionization gauges.

#### Ion Source

The ion source is of the Heil type with aperture extraction perpendicular to the cathode-anode axis. The ionizing electrons are produced by a directly heated tungsten filament. A longitudinal magnetic field is applied parallel to the cathode-anode axis to increase the effective electron paths. Typical operating conditions are: source pressure approximately  $1 \mu$ , discharge current 10 mA, anode potential +26 V, total beam current delivered to the target  $10^{-8}$  to  $10^{-9}$  A at 500-eV energy (situated at a linear distance of approximately 30 in. from the extractor electrode). The energy spread of the beam is approximately  $\pm 1$  eV at half-maximum

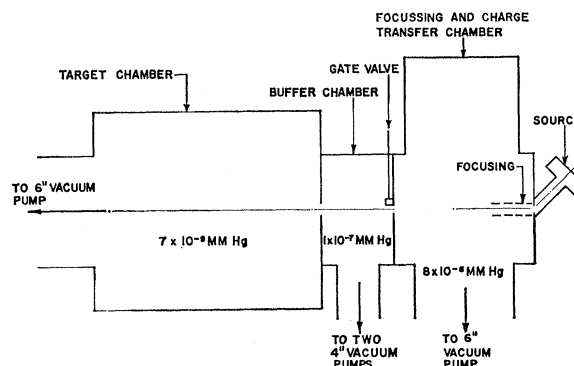


FIG. 1. Schematic diagram of the vacuum assembly. Pressures given are with source operating and beam being admitted to target chamber.

\* Supported in part by AF19(604)5554, Advanced Research Projects Agency W. O. 42-61.

<sup>1</sup> H. D. Hagstrum, Phys. Rev. 104, 672-683, (1956) and Rev. Sci. Instr. 24, 1122, (1953).

<sup>2</sup> V. G. Telkovskii, Proceedings of the Venice Conference on Ionization Phenomena in Gases, 1957 (unpublished), p. 1079.

<sup>3</sup> L. N. Large and W. S. Whitlock, Proc. Phys. Soc. (London) 79, 1948 (1962).

of the energy distribution curve. The ion beam is mass analyzed with an electromagnet with the source offset  $23^\circ$  from the axis of the apparatus. Focusing of the beam after mass separation is obtained by an Einzel lens in the source chamber.

Using commercial grade gases in the source, the ion beam shows a few subsidiary peaks. The resolution of the bending magnet is sufficient to select the appropriate species from the composite beam of ions.

### Target and Electron Collector Assembly

A flange supporting the target-collector assembly and the auxiliary electrical feedthroughs bolts on one face of the main vacuum chamber. The target  $T$ , as shown schematically in Fig. 2, is a ribbon 0.001 in.  $\times$  1.25 in.  $\times$  0.5 in. mounted in the center of the 5-in.-diam spherical collector  $C$ . The target is connected to feedthroughs on the flange by heavy copper rods which enter the sphere through a 2-in. diameter pumping hole behind the target. The rods provide a path for the flashing and ion currents. The collector is made of two hemispheres, gold-plated inside for uniform surface characteristics. The disks  $D_F$  and  $D_R$  are to collimate the beam, to prevent spurious electrons from striking the collector and to prevent secondary electrons from the target from escaping through the front orifice of the collector. Both disks have tapered orifices of  $\frac{1}{4}$ -in. diameter. The orifice of the collector is  $\frac{5}{16}$ -in. diameter.

If the currents measured at the target and collector be  $I_T$  and  $I_C$  respectively, then the secondary electron yield  $\gamma = I_C / (I_T + I_C)$ .

### Saturation Characteristics of Target Collector System

In order to ensure that all the secondary electrons ejected from the target are received on the collector and no electrons, either from the primary beam or from the two collimating disks, manage to reach it, the potential distribution shown in Fig. 2 was adopted.

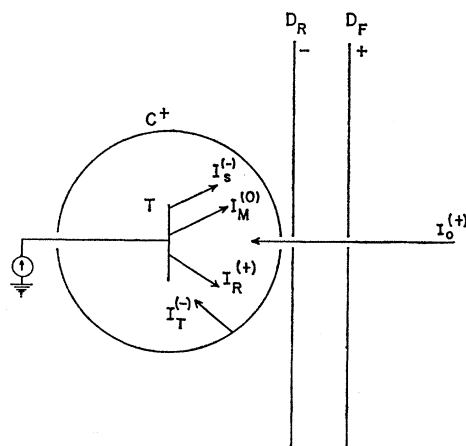


FIG. 2. Schematic diagram of target-collector system.

Maintaining the collimating disks  $D_F$  at a positive potential and  $D_R$  at a negative potential, it has been shown that (1) electrons in the primary beam do not reach the target-collector system, (2) no secondary electrons are lost from the beam aperture of  $D_F$  due to the positive potential on it, (3) secondary electrons ejected from the orifices at  $D_R$ , if any, are attracted by the potential on  $D_F$ , and (4) the secondary electrons ejected from the target along the beam axis are repelled by the field at the entrance aperture resulting from the negative potential on  $D_R$ .

### EXPERIMENTAL PROCEDURE

#### Degassing Procedure

The target is flashed by passing alternating current through it from a high-current, low-voltage transformer. The procedure adopted is to flash the target several times successively until the pressure in the target chamber drops below  $1 \times 10^{-8}$  Torr within seconds after the flash. After this preliminary processing, the flashing current is maintained at the required value for 15 sec before cutting off. Time is reckoned from this instant and the target and collector currents are observed at 15-sec intervals for about 6 or 7 min beginning with the first measurement at 15 sec. Figure 3 shows the variation of the electron yield with the flashing temperature. Each point on the curve represents a determination of  $\gamma$ , 15 sec after flashing the target to the appropriate temperature. All final yield measurements on Mo have been made after flashing the target at the maximum temperature shown in the figure, about 2000°K. The flashing temperature is estimated with an optical pyrometer in an auxiliary vacuum system.

#### Adsorption Measurements and Procedure

A quantitative measure of contamination of the target is afforded by the rate of adsorption of gas upon it. This, in turn is given by the rise in pressure,  $\Delta p$ , when the target is suddenly outgassed. If the temperature of outgassing is high enough to remove all impurities, then the surface is rendered clean the instant after a flash and maintained partially clean for a length of time depend-

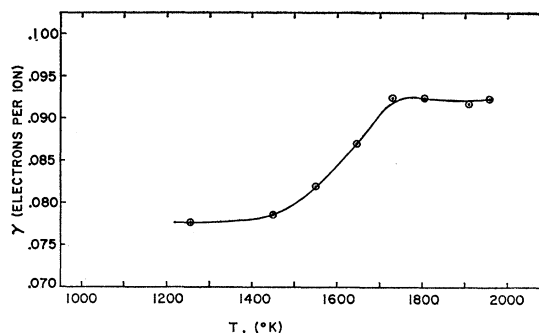


FIG. 3. Secondary electron yield for molybdenum as a function of flashing temperature.

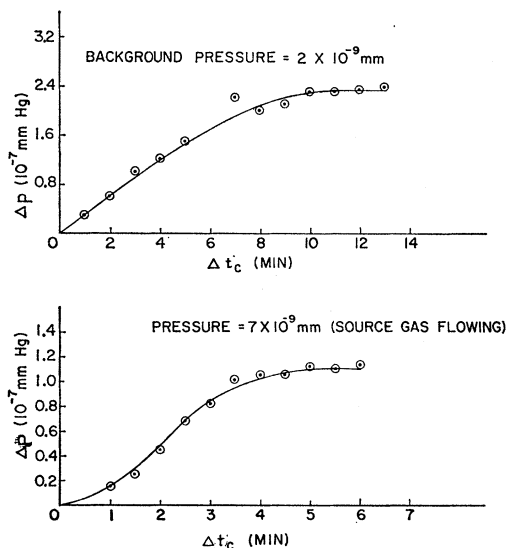


FIG. 4. Estimation of monolayer formation time for molybdenum.

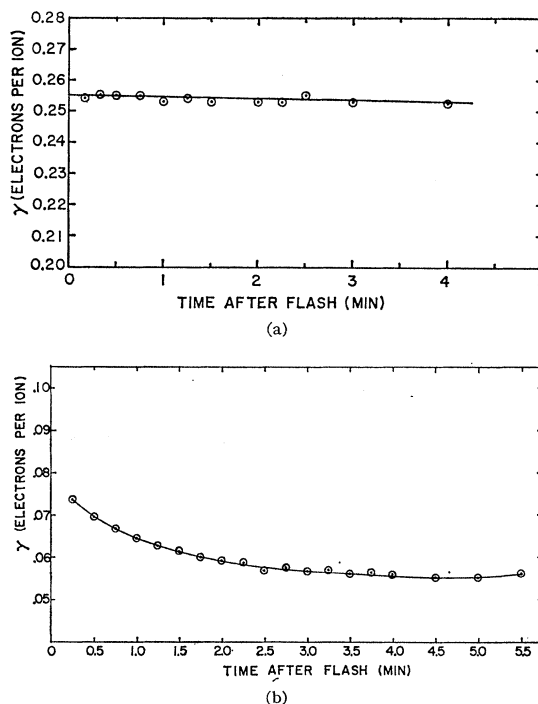
ing upon the arrival rate of molecules on the surface from the ambient and the integrated probability, " $\alpha$ ," that an incident molecule will remain on the surface (sticking probability).

Langmuir's model of adsorption on definite sites predicts a distinct change in the rate of adsorption on the surface, once the allowed sites are all occupied. Also, Becker<sup>4</sup> points out that a decrease in the sticking probability amounting to three orders of magnitude is possible for a system like nitrogen on W when the coverage changes from one monolayer to two. Therefore, if the rise in pressure  $\Delta p$  is measured by rapidly outgassing the target after various cold intervals  $\Delta t_c$ , there should be a distinct change in the slope of the  $\Delta p$  vs  $\Delta t_c$  curve. The cold interval  $\Delta t_m$  at which the slope changes should then give the monolayer formation time.

Two typical plots of  $\Delta p$  vs  $\Delta t_c$  are shown in Fig. 4, one at the background pressure of  $2 \times 10^{-9}$  Torr and the other with source gas, argon, flowing at  $7 \times 10^{-9}$  Torr. The monolayer formation times are about 12 min and 6 min, respectively. The former is consistent with a calculated maximum value of 1 sec at  $10^{-6}$  Torr.  $\Delta t_m$  at the operating pressure agrees well with that obtained by Large and Whitlock,<sup>3</sup> (for similar conditions). With He in the source, instead of Ar,  $\Delta t_m$  showed no change.

#### Estimation of $\gamma$ at the Instant After a Flash

In order to estimate the electron yield from the target immediately after a flash, the currents to the target and collector have to be measured at that instant. This is not practicable. However, by adopting the technique of Hasted and Mahadevan,<sup>5</sup> it is possible to get  $\gamma$  at  $t=0$

FIG. 5. (a) Variation of  $\gamma$  for Mo bombarded by  $\text{He}^+$  with time after flash.  $\text{He}^+$  beam energy, 600 eV. (b) Variation of  $\gamma$  for Mo bombarded by  $\text{Ar}^+$  with time after flash.  $\text{Ar}^+$  beam energy, 600 eV.

from the yield values obtained before a monolayer is formed on the target.

If  $I_F$  and  $I_G$  are the electron currents to the collector immediately after a flash and after a monolayer is formed, respectively, then

$$\log(I_F - I_G) = -\beta \Delta t_m + \log[A_0(\gamma_G - \gamma_F)],$$

where  $\gamma_F$  and  $\gamma_G$  are, respectively, the values of electron yields corresponding to the collector currents  $I_F$  and  $I_G$ ,  $A_0$  = effective current on target from the primary beam, and  $\beta = \frac{1}{4} n \bar{c} \alpha \times \sigma$ , where  $\alpha$  = sticking probability of the adsorbing species to the surface,  $n$  = number of particles/cm<sup>3</sup> in the ambient gas,  $\bar{c}$  = mean gas kinetic velocity, and  $\sigma$  = gas kinetic cross section of the adsorbing species.

Using this relation if the rate of variation of  $\gamma$  with time after flashing, until it saturates is determined, then a plot of  $\log[A_0(\gamma_G - \gamma_t)]$  versus time  $t$  would be linear, where  $\gamma_t$  = the electron yield at any instant  $t$  less than  $\Delta t_m$ . By extrapolation, the yield  $\gamma_F$  at time  $t=0$  is obtained. Typical curves showing variation of yields with time after flashing are shown in Figs. 5(a) and (b). In the case of  $\text{He}^+$ , it is seen that the yield remains practically unchanged during monolayer formation while for  $\text{Ar}^+$ ,  $\gamma$  changes significantly. Figure 6 is a semilog plot of  $(\gamma_G - \gamma_t)A_0$  versus time after flash for  $\text{Ar}^+$  of energy 600 eV.

The extrapolated value of  $\gamma$  from Fig. 6 is about 6% higher than the yield at 15 sec after flash. Likewise, the

<sup>4</sup> J. A. Becker, *Advances in Catalysis* 8, 159 (1955).

<sup>5</sup> J. B. Hasted and P. Mahadevan, *Proc. Roy. Soc. (London)* A219, 42 (1959).

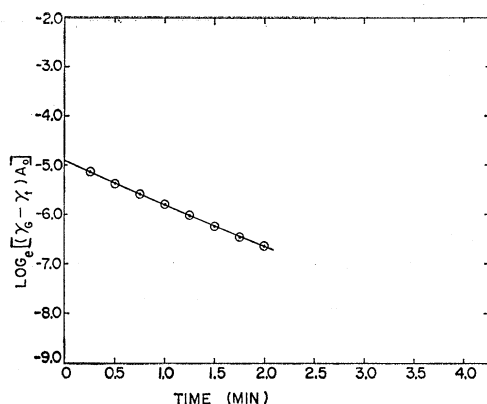


FIG. 6.  $\text{Log}[(\gamma_t - \gamma_\infty)A_0]$  vs time after flash. Energy of  $\text{Ar}^+$  beam, 600 eV.

yield for the monolayer covered surface is about 25% lower than the first value at 15 sec. In view of such rapid variation of yield with time, it is necessary to adopt the extrapolation technique for  $\text{Ar}^+$ .

The time variation of  $\gamma$  has been determined at all energies for  $\text{He}^+$  and  $\text{Ar}^+$ . For the former, the yield is unchanged even at the lowest while for  $\text{Ar}^+$ , the variation becomes less pronounced at the higher energies. The absolute yield for  $\text{He}^+$  even at the low energies is relatively large so that small variations due to partial coverage are insignificant. The same reasoning accounts for the variation becoming less pronounced at higher energies of  $\text{Ar}^+$ .

To check whether the measured value of  $\gamma$  is affected by the temperature of the target during its cooling cycle following a flash, the time variation of the yield after flashing was observed with the target at a temperature of about 500°K. Direct current heating immediately after a regular flash, using a bank of storage batteries, made it still possible to make a dc measurement of the yield. The extrapolated values of  $\gamma$  with and without this heating current agree very closely. This indicates that the secondary electron yield from clean Mo is unaffected by the temperature of the target. By using modulated beam techniques, Arifov and Rakhimov<sup>6</sup> have shown that this is true at higher temperatures as well.

By maintaining the target above ambient temperature at the normal operating pressure, the monolayer formation time  $\Delta t_m$  is in effect increased. This indicates that the integrated sticking probability of the ambient gases on the target is decreased correspondingly.

The possible presence of metastable ions in the beam was checked by varying the electron excitation energy in the source from a value below the predicted threshold energy for production of metastable ions to one above it, with the beam energy constant. The electron yield for  $\text{He}^+$  was observed to be independent of electron excita-

tion energy from 150 eV down to 60 eV. The normal operating potential on the anode for  $\text{He}^+$  was 130 V. Figure 7 shows the observed electron yields at various excitation energies for  $\text{Ar}^+$ . Each point on the curve represents a yield measurement 15 sec after flashing the target. The increase in yield at about 33-eV excitation energy, of about 5% indicates that there are metastable argon ions in the beam if the source is operated above 33 V and that these ions are relatively more efficient than the ground state ions in ejecting electrons. The predicted thresholds for metastable excitation of  $\text{Ar}^+$  are in the range 32 to 35 eV and for  $\text{He}^+$  about 65.4 eV.

## RESULTS AND DISCUSSION

The variation of the electron yield  $\gamma$  with kinetic energy of the bombarding ground state  $\text{He}^+$  and  $\text{Ar}^+$  is shown in Fig. 8. In the case of  $\text{He}^+$ , the yield drops as the energy increases to about 500 eV and, thereafter, increases linearly with energy up to 2.5 keV. For  $\text{Ar}^+$ ,  $\gamma$  is relatively insensitive to beam energy to about 700 eV and increases linearly at higher energies. The onset of a kinetic energy-dependent process of electron emission is observed in both cases.

In the region of energy overlap, our values of  $\gamma$  for  $\text{He}^+$  agree with Hagstrum's very well up to 500 eV and increase more rapidly at higher energies. The energy threshold for kinetic emission of electrons from the target is about 500 eV, in agreement with Hagstrum's. For  $\text{Ar}^+$ , at the low energies our values are about 25% lower than Hagstrum's. The onset of kinetic emission has not been observed by him. We are in excellent agreement with Arifov and Rakhimov<sup>6</sup> at the higher energies. We are also in good agreement with Magnuson and Carlston<sup>7</sup> who use an intense beam bombardment technique to determine  $\gamma$  for  $\text{Ar}^+$  from clean Mo. The rate of increase of  $\gamma$  with beam energy is appreciably higher for  $\text{He}^+$  than  $\text{Ar}^+$ . Petrov and Dorozhkin,<sup>8</sup> also observe that for the noble gas ions the slope decreases

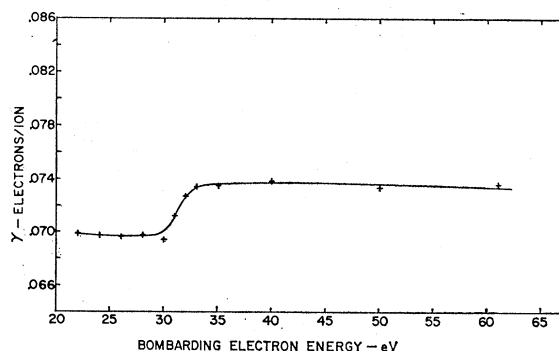


FIG. 7. Variation of  $\gamma$  for Mo bombarded by  $\text{Ar}^+$  as a function of bombarding electron energy.  $\text{Ar}^+$  beam energy, 500 eV.

<sup>7</sup> G. D. Magnuson and C. E. Carlston, *Bull. Am. Phys. Soc.* **7**, (1962).

<sup>8</sup> N. N. Petrov and A. A. Dorozhkin, *Soviet Phys.—Solid State* **3**, 38 (1961).

<sup>6</sup> U. A. Arifov and R. R. Rakhimov, *Transactions of the Ninth All Union Conference on Cathode Electronics*, Moscow, 1959 (unpublished), p. 666.

as the atomic number of the bombarding particle increases.

Parillis and Kishinevskii<sup>9</sup> have estimated a velocity threshold for kinetic emission of electrons by ions from metals, based on their ion-atom collision model for transfer of ion kinetic energy to electrons in a metal. They give a velocity between  $0.6$  and  $0.7 \times 10^7$  cm per sec for the bombarding ion. In the case of  $\text{Ar}^+$  on Mo, the velocity threshold observed by us is in excellent agreement with this computed value. Very reasonable concurrence with this velocity threshold has been reported for heavy ions  $\text{Ar}^+$ ,  $\text{Kr}^+$ ,  $\text{K}^+$ , and  $\text{Mo}^+$  bombarding W and Mo.<sup>9</sup> This estimate of threshold velocity is valid only for ion-metal pairs satisfying the inequality  $\frac{1}{4} < Z_1/Z_2 < 4$  where  $Z_1$  and  $Z_2$  are the atomic numbers of incident and target atoms, respectively. The inequality is not valid for  $\text{He}^+$  incident on Mo. The kinetic emission threshold for  $\text{He}^+$  observed by us and Hagstrum is around 500 eV corresponding to a velocity of  $1.5 \times 10^7$  cm per sec, which is consistent with the model. The velocity thresholds obtained by extrapolation by Telkovskii for  $\text{He}^+$  and  $\text{Ar}^+$  incident on Mo are about  $2 \times 10^7$  cm per sec and  $1.5 \times 10^7$  cm per sec, respectively. However, the extrapolation is not justified since at low energies near the kinetic threshold,  $\gamma$  varies linearly with energy and not with ion velocity. This is what we observe and what Parillis *et al.* predict.

A crude estimation of the kinetic energy of the incident particle at which the electron yield is maximum was made on the basis of Massey's<sup>10</sup> adiabatic hypothesis for inelastic collisions involving electronic transitions. This estimation is justifiable only because the curves of yield vs energy of incident particles for various ion-metal pairs do show, in general, flat maxima at higher energies.<sup>3,11</sup> The lowest estimates of kinetic energy for  $\text{He}^+$  and  $\text{Ar}^+$  incident on Mo are 5 and 10 keV, respectively. Both these are beyond the range of our measurement. Therefore, the observed increase of  $\gamma$

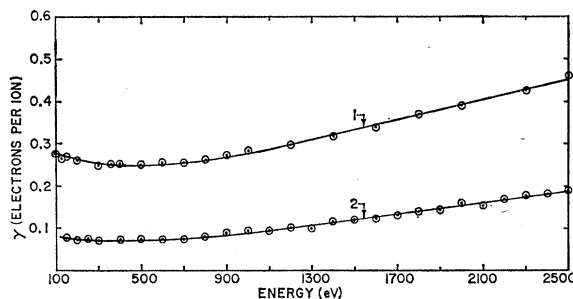


FIG. 8. Secondary electron yield,  $\gamma$ , for clean molybdenum as a function of kinetic energy of incident ions. 1— $\text{He}^+$ , 2— $\text{Ar}^+$ .

with energy is not inconsistent with the ionization model of Parillis *et al.*

Hagstrum and Arifov have heated the polycrystalline target material at a temperature of order  $2000^\circ\text{K}$  for hours at a stretch (8 to 18 h for Arifov). It is quite possible that by annealing the sample at this temperature, a large-grained structure has been formed,<sup>12</sup> the temperature of annealing being much higher than the recrystallization temperature for Mo ( $900^\circ\text{C}$ ). The total flash duration on each sample of target material used in our measurement is of the order of 1h, made up of several 15-sec flashes at about  $2000^\circ\text{K}$ . The target invariably burns out at the end of such a cycle of flashes. The target samples would thus be more randomly oriented than the ones annealed at high temperature. If the absolute yield for an ion-metal pair be comparatively small as for  $\text{Ar}^+$  on Mo, then the differences in randomness of orientation of the target could show up small differences in electron yields as well. Such spreads would be insignificant when the total yield is large.

#### ACKNOWLEDGMENTS

Our thanks are due to Dr. F. C. Hurlbut and W. C. Crocker for designing and building the vacuum system, to P. A. Kinzie and R. D. Moore for building the ion source, and to A. R. Comeaux for technical assistance in the operation of the apparatus.

<sup>12</sup> *Metals Handbook*, edited by Taylor Lyman (American Society for Metals, Cleveland, Ohio, 1960), p. 1140.

<sup>9</sup> E. S. Parillis and L. M. Kishinevskii, *Soviet Phys.—Solid State* **3**, 885 (1960).

<sup>10</sup> H. S. W. Massey and E. H. S. Burhop, *Electronic and Ionic Impact Phenomena* (Clarendon Press, Oxford, 1952), p. 441.

<sup>11</sup> E. J. Sternglass, *Phys. Rev.* **108**, 1 (1957).